Study of Surface and Bulk Electronic Structure of II–VI Semiconductor Nanocrystals Using Cu as a Nanosensor

G. Krishnamurthy Grandhi,[†,#] Renu Tomar,[†,‡,#] and Ranjani Viswanatha[†,‡,*]

[†]New Chemistry Unit and [‡]International Centre for Materials Science, Jawaharlal Nehru Centre for Advanced Scientific Research, Jakkur, P.O., Jakkur, Bangalore 560064, India. [#]These two authors contributed equally to the work.

ABSTRACT Efficiency of the quantum dots based solar cells relies on charge transfer at the interface and hence on the relative alignment of the energy levels between materials. Despite a high demand to obtain size specific band offsets, very few studies exist where meticulous methods like photoelectron spectroscopy are used. However, semiconductor charging during measurements could result in indirect and possibly inaccurate measurements due to shift in valence and conduction band position. Here, in this report, we devise a novel method to study the band offsets by associating an atomic like state with the conduction band and hence obtaining an internal standard. This is achieved by doping copper in semiconductor nanocrystals, leading to the development of a characteristic intragap Cu-related emission feature assigned to the transition from the conduction band to the atomic-like Cu *d* state. Using this transition we determine the relative band alignment of II–VI semiconductor nanocrystals as a function of size in the below 10 nm size regime. The results are in excellent agreement with the available photoelectron spectroscopy data as well as the theoretical data. We further use this technique to study the excitonic band edge variation as a function of temperature in CdSe nanocrystals. Additionally, surface electronic structure of CdSe nanocrystals have been studied using quantitative measurements of absolute quantum yield and PL decay studies of the Cu related emission and the excitonic emission. The role of TOP and oleic acid as surface passivating ligand molecules has been studied for the first time.

KEYWORDS: nanocrystal band offset · Cu doping · II–VI semiconductors · surface trap states · photoluminescence

The study of the electronic structure of nanocrystals plays an important role in tailoring the band offsets to maximize the degree of overlap between the wave functions[1] and in various applications like the excitonic solar cells[2] along with the acquisition of high quality nanocrystals.[3] One of the key factors governing the efficiency of the solar cells is the interfacial electronic energy alignment which is important to accurately determine the electronic energy offsets in nanocrystals.[4,5] In addition, the success of using organic ligands in the manipulation of surface electronic properties of the colloidal nanocrystals has largely been responsible for the various applications of these nanocrystals.[6–10] Recent studies have shown that surface charging, which can be accurately controlled by the knowledge of the ligands present on the surface and their function, plays an important role in quantitative and qualitative understanding of the surface excitonic effects leading to multiexciton generation.[11–14] Nevertheless, the study of the surface electronic structure has been rather elusive apart from a few works,[8–10] and the choice of ligands used to design an efficient nanocrystal, till date, has mostly been carried out intuitively. Ligands are often known to perform multiple activities like passivating a hole trap while creating an electron trap and hence the actual concentration and functions of the ligand are important for the acquisition of optimal passivation of the surface.[6,9] An in-depth understanding of the bulk and surface electronic structure in nanocrystals greatly enhances our capability of obtaining high quality nanocrystals and using them more effectively in potential applications.

It is well-known for a long time that the band gap of the nanocrystal varies as a function of size, and several techniques, particularly absorption spectroscopy, have been used extensively to study the evolution of the bandgap of these materials.[15] Cyclic voltammetry, that is more compatible

* Address correspondence to rv@jncasr.ac.in.

Received for review July 19, 2012 and accepted October 17, 2012.

Published online October 17, 2012
10.1021/nn304149s

with organic ligands, has been useful in finding out the absolute positions of band edges in bulk with respect to vacuum using ionization potential and electron affinity.[16−18] However, along with specific concerns about solvent, electrode, and electrolyte, it is not quite straightforward to obtain the shift in conduction band (CB) and valence band (VB) of the nanocrystals from the ionization potential since the optically observed excitonic band gap is not related to the ionization potential and electron affinity in a direct manner.[19] More recently, a rapid technique known as the photoelectron spectroscopy in air has been introduced to determine the ionization potential on films and powder. While this technique has been used to determine the VB and CB variation as a function of size in quantum dot samples,[19] it is evident that it involves a substantial number of assumptions to derive the CB and VB shift including the effective mass approximation and an arbitrary assumption of the dielectric constant of the matrix. Clearly, although extensive research has been devoted for the study of size-dependent evolution of CB and VB *via* experiment, deconvolution of the shift in CB and VB in nanocrystals has mainly been dominated by theoretical results.[20−25] Nevertheless a few examples exist wherein the position of the band edges have been determined using photoemission spectroscopy,[26−30] X-ray absorption spectroscopy,[29] or scanning tunneling spectroscopy.[31] These methods, while providing the basis for the experimental realization of the isolated study of evolution of CB and VB has major limitations in terms of experiment. Both photoemission and X-ray absorption spectroscopy and most often scanning tunneling spectroscopy have to be carried out in ultrahigh vacuum that makes these measurements very extensive and time-consuming.[28] Additionally inaccuracies in the energy positions set in because of the problems of charging of the semiconductor nanocrystals.[26,28,32] Because of the presence of surface organic ligands, the samples may also be damaged in the beam or may degas extensively.[32] Hence development of a simple alternate method that is organic ligand friendly, less time-consuming, and straightforward to measure is necessary to accurately map the CB and VB positions in the nanocrystals. The presence of such a method has an additional important consequence in the study of heteronanostructures. Currently, because of the absence of extensive data for the band offsets as a function of size, it has been generally assumed that the band alignment in nanocrystals follows the same trend as that of bulk materials. Consequently, it would not be possible to determine the presence of band crossings, if any, although it would drastically affect the properties of the heterostructure in question. The measurement of band offsets for a large number of sizes in various nanocrystals opens up a new arena of study in the field of nanocrystal heterostructures.

In this paper, we introduce a novel way of measuring band offsets by doping small amounts of Cu into the nanocrystal and studying the emission from the CB to the atomic-like Cu d level. This method, along with being a more direct probe that can be performed at atmospheric conditions with a simple optical measurement also has an additional advantage of being a nanosensor present permanently in the nanocrystal. It is well-known in literature that band offsets vary as a function of size, temperature, and ordering.[33,34] This technique allows us to study the band offsets as a function of temperature as well as in large scale assemblies thus acting as an excellent sensor to study the bulk electronic structure of the nanocrystal. In this manuscript, we have first used CdSe as a model system to study the variation of band offsets as a function of size. Further we not only prove the generality of the proposed method by extending this technique to other II−VI semiconductors but also use this technique to determine the relative band alignment in II−VI semiconductor nanocrystals. Interestingly, we show for the first time that while band alignment in bulk can be extended to nanocrystals in the study of VB, it is not true in the case of CB. Consequences of these band crossings have also been explored in this manuscript. Introduction of Cu to study the electronic structure of the host NC has far-reaching consequences. For example, we can study the variation of band edges as a function of temperature as discussed in this manuscript leading to the discovery of interesting effects that have not been observed earlier. Furthermore, by means of the quantum yield (QY) and the PL decay dynamics of the Cu related emission and the excitonic band edge (BE) emission of doped and undoped nanocrystals we have demonstrated for the first time that it is possible to study the role of the ligand in surface passivation and hence facilitate the acquisition of optimally passivated nanocrystals.

RESULTS AND DISCUSSION

Copper doping of semiconducting nanocrystals has been extensively explored in several recent reports.[35−40] One common trend emerging from these studies is the presence of the characteristic long-lived intragap Cu-related photoluminescence (PL) band accompanied by suppression of the intrinsic BE emission. It is well-known in the community that impurities like Cu,[35−39,41] Eu,[41−44] Co,[45,46] or Mn[41,47−49] introduce atomic-like states within the forbidden gap of the host semiconductor that can exchange charges with the VB and CB *via* radiative and nonradiative transitions. While the mechanism of this intragap luminescence in Cu has been extensively debated in several recent reports,[36,38,39] the origin of this wide band has been universally accepted and has been attributed to the optical transition from the CB of the host semiconductor to the atomic-like Cu d level. It has been extensively proven in literature that energies of atomic levels with respect to vacuum are independent of the host semiconductor (for example, Mn d−d transition at

2.15 eV,[41,47,48] or Eu $^5D_0 - {}^7F_2$ transition at ~2 eV[41−44]) and size.[46,49] However in most of these cases optical transition has been observed from atomic level to atomic level and hence cannot be used to determine the electronic structure of the host. The presence of a single Cu d level in the midband gap region presents us with a unique opportunity to measure the association of an atomic state with the CB of the host semiconductor providing an important internal standard[50] to study the shift in the CB as a function of size and as a function of various host materials. A compilation of available literature[51−56] on the band alignment as well as Cu levels in bulk semiconductors is shown in Figure 1a. Analogous to the other transition metal and lanthanide energy levels arising from atomic states, it is evident that the Cu level also remains constant within ±0.05 eV from one semiconductor to another in the bulk regime (see also the Supporting Information). Similarly, as shown by earlier theoretical results for Mn[49] and experimental and theoretical results for Co and other impurity levels,[46] one would expect that the same would be true as a function of size for the Cu d levels. The schematic representing the transitions from the CB to the Cu d level in addition to the band gap transition under this assumption is shown in Figure 1b. If this assumption was indeed true, it would be possible to independently investigate the shift in the CB of the host nanocrystals as a function of size by determining the position of the Cu related PL peak.

While the position of the Cu related emission can be used to determine the shift in the CB, it is fascinating to note that the QY and the lifetime dynamics of the Cu related emission can be effectively used as a direct probe to study the surface electronic structure of the nanocrystals. Consequently, with an intention of accomplishing this, we initially try to understand the mechanism of PL decay of the Cu related emission in doped nanocrystals. In order to elucidate the actual mechanism of emission from CB to the Cu d level, it is important to determine the oxidation state of Cu. While some early papers attribute the intragap luminescence to the Cu^{1+} state[39] and the reminiscent BE emission to the fraction of undoped dots, recent results have proved otherwise.[38] Using magnetic circular dichroism, Klimov *et al.*[38] have shown that Cu is indeed in the 2+ oxidation state and hence acts as a permanent optical hole. This implies that Cu emission can be activated in the absence of a photogenerated hole (Figure 1c). Nevertheless, since this emission is known to be several orders of magnitude slower than the BE transition, the emission would be dominated by the BE transition[38] (Figure 1d), if the photogenerated holes are not lost by some mechanism like, for example, the surface hole traps. Therefore the intensity ratio of emission and the lifetime decay studies of Cu emission give important information regarding the presence of surface electron and hole traps and can be used to study the surface electronic structure of the nanocrystal, thus contributing to our understanding of the role of various ligands in passivating the surface.

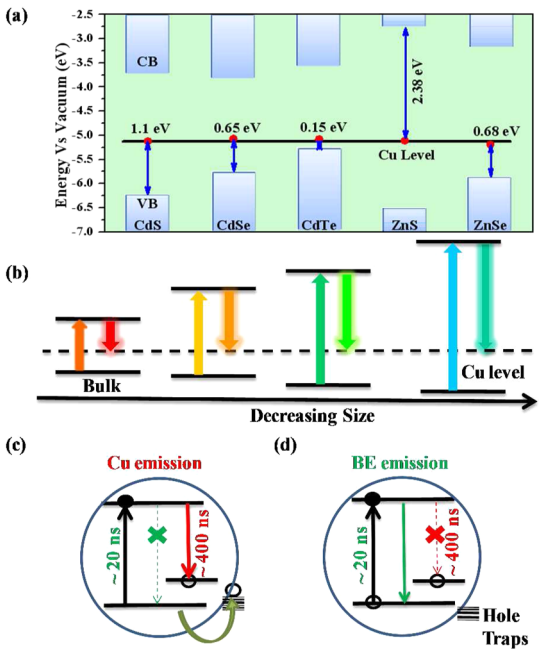

Figure 1. (a) Bulk band gap and position of the Cu state in CdS, CdSe, CdTe, ZnS, and ZnSe. The relative bulk band alignment[51,52] and the Cu state positions[53−56] are collected from various literature references. (b) Schematic of the energy level diagram showing the variation of the CB, VB, and the Cu d level with decreasing size. Schematic of the energy level diagram of the nanocrystals containing Cu^{2+} ions in unpassivated (c) and passivated (d) crystals showing the presence of Cu-related emission and the BE emission.

We have used CdSe nanocrystals as a model system to study the electronic structure since it has been one of the most widely synthesized nanocrystals in literature with narrow size distributions and excellent optical stability. However, doping CdSe with various dopants including Cu has been tried by different groups which led to it being classified as undopable[57] based on the absence of Cu emission peak in the optical spectrum. Reasons for this were attributed to intrinsic self-purification to fundamental thermodynamic or kinetically controlled processes such as the crystal structure.[7,35,57] In this manuscript, we demonstrate that the presence or absence of PL emission attributed to Cu states does not determine the efficacy of doping in nanocrystals. For example, in this specific case of CdSe, we illustrate that it is possible to obtain the emission from the CB to the copper d state by systematically varying the ligands to alter the surface of the nanocrystal. A logical route to the synthesis and characterization of Cu-doped CdSe with a prominent emission from CB to the Cu d level has been established by systematically varying the surface ligands.

Cu doped CdSe nanocrystals were synthesized using cadmium oleate ($CdOl_2$) as the Cd source and trioctylphosphine (TOP) complex of Se (TOPSe) as the Se

source. The details of the synthesis are given in the Methods section. Cu stearate in octadecene (ODE) solution was injected into the solution after the formation of CdSe, the amount of Cu being determined such that the solution did not precipitate when heated at high temperatures. The formation of nanocrystals was characterized using X-ray diffraction (XRD) measurements. Typical XRD patterns of doped and undoped CdSe are shown in Figure 2a. Comparing the XRD patterns with that of the bulk CdSe, crystallizing in zinc blende and wurtzite structures, we observe that both doped and undoped nanocrystals crystallize in the same cubic zinc blende phase with similar lattice parameters. Similar to earlier literature reports, the pattern was simulated[58] (also shown in Figure 2a) by broadening the bulk XRD pattern using the Scherrer formula, and quantitative information on the size of the nanocrystals was obtained. The size of the nanocrystals obtained by this procedure for both doped and undoped samples was found to be 2.5 nm implying that the size and crystal structure did not change after doping Cu. In the earlier literature, there was a debate[7] on the viability of doping based on the crystal structure of the nanocrystal, and it was concluded that the nanocrystal can only be doped if it is formed in the cubic phase. Thus our nanocrystals should be ideal candidates to dope with Cu. Nanocrystal sizes were also confirmed using transmission electron microscopy (TEM), and a typical TEM image is shown in Figure 2b which shows an abundance of spherical particles with sizes in agreement with XRD results. Selected area electron diffraction (SAED) shown in the inset to Figure 2b as well as lattice fringes seen in these particles confirms a high degree of crystallinity of the sample as is also evident from the XRD patterns. The amount of Cu present in the sample was measured using inductively coupled plasmon optical emission spectroscopy (ICP−OES). Cu doped CdSe nanocrystals synthesized using a standard technique using TOP, trioctylphosphine oxide, oleic acid (OlAc), and octadecyl amine as ligands, synthesis being discussed as the standard technique in the Methods section, showed no incorporation of Cu in CdSe as determined by the absence of the red-shifted PL peak as well as ICP−OES data. The XRD data (Figure S1 in Supporting Information) shows that the nanocrystal crystallizes at least partially in the wurtzite structure. Further studies into these nanocrystals indicated that the BE QY of these samples were found to be quite high (*ca.* 6−10%) and should have been well passivated. In the light of earlier investigations in the case of Cu doped in the ZnSe/CdSe system,[38] it has been shown that the CB to Cu d level emission is several orders of magnitude slower compared to the BE emission and hence requires a surface hole trap to remove the photogenerated hole thus creating a pathway for the Cu related emission. Consequently to observe the red-shifted PL emission, it is necessary to increase the hole traps during the synthesis of the nanocrystal. This is achieved by studying the chemistry of the ligand molecules.

In this case in order to isolate functions of the various ligands, we have restricted the ligands to only TOP and OlAc though they are known to give a low PL quantum yield, and the synthesis method is discussed under the heading of limited ligands method in the Methods section. TOP has a P atom with a lone pair of electrons giving rise to some extra electron density on the P atom. This electron density, in principle should be capable of passivating the hole in the VB of the nanocrystal if its absolute energy level is above the VB of the nanocrystal.

Typical PL and absorption of doped and undoped nanocrystals are shown in the inset to Figure 2c. It is important to note here that "as obtained" spectrum of doped nanocrystals do not result in the spectrum shown in Figure 2c. Since the Cu related emission is broad and occurs in the 600−800 nm regime where most detectors are known to have decaying efficiencies we obtain a Cu peak that is weak as a consequence of the artifact of decaying detector efficiency (shown in the Supporting Information, Figure S2a). Fortunately, since CdSe nanocrystals emit in the visible region, a visual inspection of the doped and undoped sample (Supporting Information Figure S2b,c) clearly showed that the as obtained spectrum needs to be corrected. Additionally, since we are interested in studying absolute energy of the host nanocrystal, we have also applied the necessary energy correction[59] as shown in Figure S2d to arrive at the final spectrum that will be referred to as PL spectra for future references. Here on comparison of the PL spectra (red line) with undoped CdSe, we observe the presence of a weak PL feature at ∼1.63 eV that is red-shifted relative to the BE absorption feature, and a strong residual BE emission peaked at about 2.25 eV. However, ICP−OES analysis of the extensively washed sample shows the presence of substantial Cu within the nanocrystal. Upon incorporation of copper, the ratio of the red-shifted PL peak relative to the BE absorption feature has traditionally been used to determine the extent of success in integrating the Cu atom into the lattice of the nanocrystal.[39] However, PL lifetime studies shown in the main panel of Figure 2c, collected at both the spectral features shows that the Cu related emission is several orders of magnitude slower than the BE emission similar to the earlier reports,[38] and hence the intensity ratio of the Cu related PL emission cannot be used as a direct measure of the capability to dope Cu into the lattice of the nanocrystal. The BE emission lifetime is found to be about ∼20 ns while the Cu^{2+} PL lifetime is mostly single exponential with a much larger lifetime (∼500 ns), confirming that the peak is not due to the surface states and is due to the weak spatial overlap between the conduction-band electron wave function

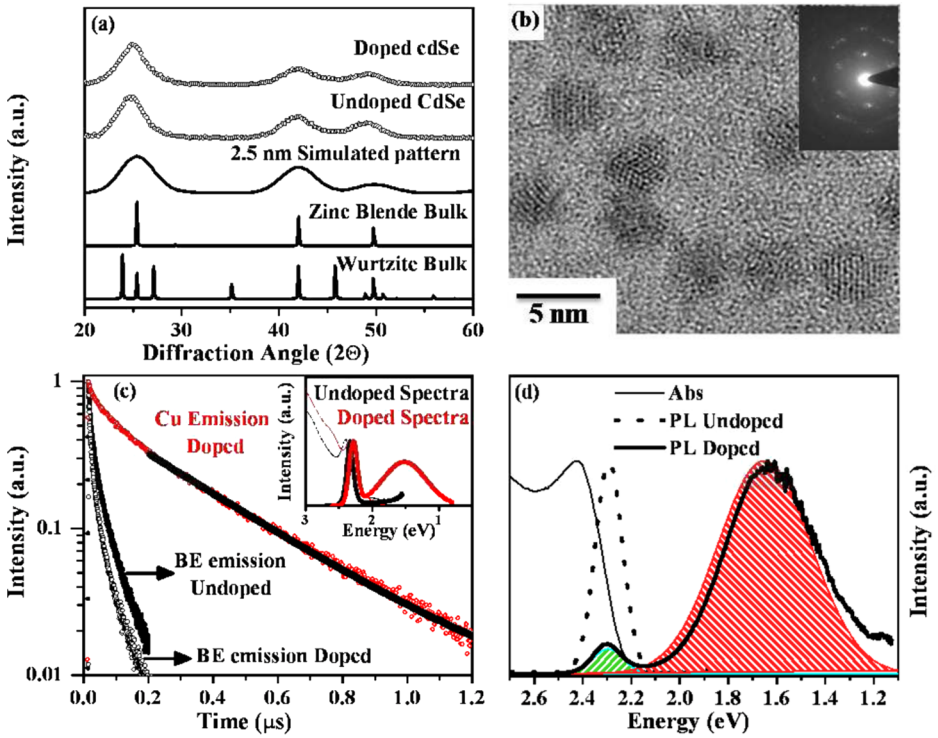

Figure 2. (a) XRD patterns of typical Cu doped and undoped CdSe nanocrystals along with the simulated pattern for 2.5 nm particle and the bulk wurtzite and zinc blende crystal structures. (b) Typical high resolution TEM of Cu doped CdSe nanocrystals. Shown in the inset is the SAED pattern of the nanocrystals. (c) Time resolved PL data of the undoped (closed circles) and doped (open circles) sample at the BE emission (black circles) and the doped sample at Cu related emission (red circles) along with a single exponential fit (black line). Inset shows the absorption and PL data for doped (red line) and undoped (black line) highly passivated nanocrystal. (d) Absorption (thin solid line) and PL spectra of doped (thick solid line) and undoped sample (dotted line) along with a typical area under the PL peaks.

and the localized copper state. Furthermore, by studying the PL decay dynamics of the Cu related emission, it is clear that though there is a fairly large component of the single exponential lifetime as shown by the fit to the experimental data (black line), it cannot be fitted to a perfectly single exponential decay. We observe that there is an initial fast decay that should be due to the surface electron trap states as the photogenerated hole is not involved in the Cu emission. Hence the percentage of the fast component in the lifetime dynamics of the Cu related emission is indicative of the amount of surface electron traps present in the nanocrystal.

From these studies, it is also clear that as long as photogenerated electron and hole recombine radiatively, we would not observe the Cu related emission. Hence we need to create hole traps while passivating the electron traps to facilitate this emission pathway. In the current case, this hypothesis is further validated by reducing the amount of TOP used during the synthesis of the nanocrystal. A typical PL spectrum obtained by drastically reducing the TOP concentrations during the reaction but with similar Cu concentration is shown in Figure 2d. Here we observe the presence of an intense PL at ~1.63 eV (shaded red) and a weak residual BE emission peaked at about 2.25 eV (shaded green), thus validating the hypothesis that TOP indeed acts as a hole passivating molecule. The quantum yield (QY) of the emission at ~1.63 eV was found to be quite high (~15%) and was also red-shifted compared to the surface state emission position (~1.8 eV) thus confirming that this peak is not due to the surface states. XRD and TEM were carried out to confirm that there was no change in structure or size of the host nanocrystal upon incorporation of Cu in the nanocrystal. Hence the study of PL QY and the lifetime dynamics of the Cu related emission provide us with a unique probe to understand the surface of the nanocrystal in terms of electron and hole traps.

Size-dependent bulk electronic structure of the CdSe nanocrystals was explored by systematically studying the position of the Cu related emission in doped systems. The position of the Cu emission has been extensively studied prompted by the constant 2.15 eV emission of Mn d−d transition irrespective of the size or the host material. The position is observed to be red-shifted with respect to the BE emission and is tunable by tuning the size of the nanocrystal.[37,40] Similar to that of other systems studied till date, typical absorption and emission spectra of doped and undoped CdSe nanocrystals obtained for varying sizes is observed to have an intense tunable Cu related emission (Figure 3a) that is red-shifted with respect to the BE emission.

This tunability of the Cu related emission is expected since the emission occurs from the CB of the nanocrystal

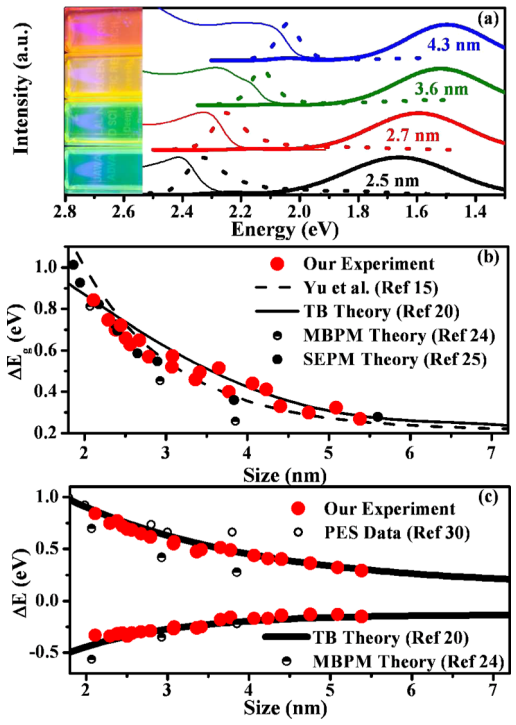

Figure 3. (a) Typical absorption and PL spectra of the doped and undoped CdSe nanocrystals for varying sizes showing a shift in the Cu related emission position. Inset shows a digital picture of Cu doped samples of various sizes. These are excited using a hand-held UV lamp at 350 nm excitation. (b) A variation of bandgap as a function of size (filled red circles) along with the TB (tight binding) (solid black line) (ref 20), MBPM (many body pseudopotential method) (half filled black circles) (ref 24), SEPM (semi-empirical pseudopotential method) (filled black circles) (ref 25) theoretical techniques and other experimental results (dotted black line) (ref 15). (c) Variation of VB and CB shift in bandgap obtained from analyzing the Cu related emission shown as filled red circles overlapped with the TB (solid line) (ref 20), MBPM (half filled black circles) (ref 24) theoretical techniques and from photoemission (open black circles) (ref 30).

to the atomic-like Cu d level and the CB is known to shift as a function of size. However, it is important to note that since the Cu d level is not expected to shift as a function of size, the shift in the position of the Cu related emission is entirely due to the shift in the CB of the nanocrystal and hence allows us to have a novel method to separately probe the CB and VB of the nanocrystal. Hence taking extensive care to correct the wide Cu related PL emission spectra with the necessary grating efficiency and energy correction to determine the exact PL maxima of the Cu related emission, we have used the Cu related emission maxima to determine the shift in the CB. Typical variation of the bandgap of the nanocrystal as a function of size is shown in Figure 3b while the variation of CB and VB as obtained from the Cu emission position is shown as filled circles in Figure 3c. The solid line shows the values obtained from semi-empirical tight binding (TB) model[20] for the theoretical prediction of bandgap and the VB and CB variation of CdSe nanocrystals. In the case of CB and VB variation, the theoretical prediction is calculated by subtracting the entire coulomb correction term from the CB and shifting the experimental value of the VB position of the largest nanocrystal to match the theoretical value. With this one arbitrary shift, it is found that the experimental data obtained from Cu related emission position shows an excellent agreement with the theoretical values as shown in Figure 3c. The open symbols were obtained from literature where the position of CB was obtained using time-consuming photoemission spectroscopy and X-ray absorption measurements.[30] The excellent agreement with these experimental data as well as theoretically predicted values proves that the Cu level is independent of size and that this technique can indeed be used to measure the shift in the CB of the nanocrystal.

The determination of relative band alignment of various semiconductors is a natural consequence of the simplicity and the ease of this technique. This allows us to acquire a large number of data points by obtaining varying sizes of the doped nanocrystals with different host materials. Hence we first went about this by synthesizing various Cu doped semiconductor nanocrystals. The synthesis techniques are described in the experimental section, and the samples were characterized using TEM, XRD, ICP-OES, and absorption and PL techniques. PL data showed the presence of a strong Cu related emission in every case. To prove the validity of the approach mentioned above, we quantified the shift in the Cu related emission and obtained the CB and VB variation for various semiconductors and plotted them as a function of size along with the theoretical curves and other experimental data, when available, in literature as shown in Figure 4. While the extremely good agreement with the theoretical data as well as photoemission data from earlier literature[27,60,61] in all cases proves the generality of this approach it would be more instructive to obtain the relative band alignment of the host semiconductors in the nanosize regime. Figure 5a shows the absorption and PL data for the 3.8 nm doped and undoped semiconductor nanocrystals. It is interesting to note that the relative intensities of BE emission and Cu related emission as well as the shift in the position of the Cu related emission shows a wide variation from one semiconductor to another. From the figure it is evident that the shift in the position of the Cu related emission for the same size nanocrystal varies from 0.2 to 1.3 eV as expected from the above mechanism. The relative intensity of the Cu related emission depends upon the number of surface trap states associated with the host material[38,62] and is discussed in greater detail later in the text. However, it is important to quantify the CB and VB variation to find out if the bulk alignment is valid in the nanocrystal regime. Towards this end, we subtracted the theoretically obtained energy of the band offset at 9 nm in every case and plot the CB variation (main panel) and the VB variation (inset) in Figure 5b for the various semiconductors.

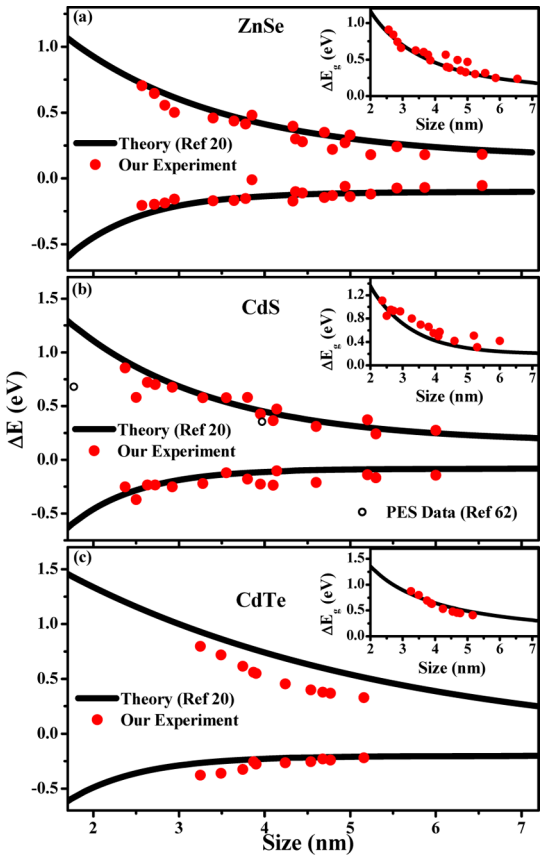

Figure 4. The main panels show the CB and VB variation as a function of size as obtained from the analysis of Cu doped nanocrystals (filled red dots) along with TB theoretical curve (solid lines) and data obtained from PES data from literature (black open circles) for (a) ZnSe nanocrystals, (b) CdS nanocrystals, and (c) CdTe nanocrystals. The insets show the corresponding band gap variation as a function of size.

It is interesting to note that while the VB follows a universal curve and can hence be translated from the bulk, the CB alignment changes drastically from that of the bulk semiconductors. Hence we plot the actual band offsets of the CB (Figure 5c) and VB (Figure 5d) as a function of size keeping the vacuum level as a single reference. Figure 5c clearly shows that the band alignment changes as a function of size in nanocrystals leading to interesting band crossings. For example, it can be seen that while 3 nm CdTe and ZnSe have the CB at the same energy, the CB of 6 nm ZnSe lies 270 meV higher than similar sized CdTe as compared to 400 meV in bulk semiconductors. These relative alignments as a function of size are important in understanding the optical properties of core–shell heterostructures that subsequently determines the efficiencies of various absorption and emission based devices.

The shift in the CB as a function of temperature or ordering can also be measured using this technique due to the presence of an internal standard. For example, Figure 6a shows the shift in the bandgap as a function of temperature for two different sizes. The solid lines show a fit to temperature dependence of the bandgap to the Bose–Einstein model[63] given by

$$E_g(T) = E_g(0) - \frac{2a_B}{\exp\left(\frac{\theta}{T}\right) - 1} \quad (1)$$

where a_B is the strength of the electron phonon interaction and θ is the temperature corresponding to the average energy of the phonons involved in the process. The equation fits well to the excitonic band gap values obtained for both the sizes, and the θ for the 2.4 nm particle was found to be 369 K and that for 3.3 nm particle was found to be 220 K. The bulk value is reported to be 179 K[64] and the simulated curve is shown in the figure. Thus it can be seen that the average energy of the phonons involved in the bandgap transition increases with a decrease in size. A careful study of the variation of excitonic band gap as well as the Cu related emission at varying temperatures as shown by a typical PL spectra at 300 K and at 80 K in Figure 6b suggests that the shift in the Cu related emission is less than that of the band edge exciton as well as with varying intensity ratio. While the varying intensity ratio will be discussed later in the text, Figure 6c shows the shift in Cu emission for the 2.4 nm particle as well as the difference between the excitonic band gap shift and the Cu emission shift, giving us a direct probe to study the shift in the CB and VB as a function of temperature for the first time. It can be seen that the variation of CB and VB as a function of temperature is non-monotonic unlike that of excitonic band edge variation. This could be due to the complex interplay of the bandwidth and band center as a function of temperature resulting in a nonmonotonic band edge dependence. However one needs more theoretical studies to quantitatively understand these dependencies that is beyond the scope of the current manuscript. Thus Cu related emission plays an important role in understanding the bulk electronic structure of the nanocrystal under various conditions due to the presence of an internal standard.

Surface electronic structure of host nanocrystals can also be studied along with the bulk electronic structure using the Cu related emission, as already mentioned earlier in the text. To obtain more insight into the nature of the surface of the nanocrystal for any given size of the nanocrystal and hence the function of ligand molecules in passivating the surface, we varied each of the ligands systematically and studied the QY of the BE emission and the Cu related emission as well as the lifetime dynamics of these two spectral features. Traditional wisdom suggests that the presence of a larger amount of Cu within the nanocrystal increases the QY of the Cu related emission. With the intention of verifying this we measured the QY of the Cu related emission for varying amounts of Cu added stoichiometrically, the results of which are shown in the main panel of Figure 7a. The maximum amount of 0.25% of

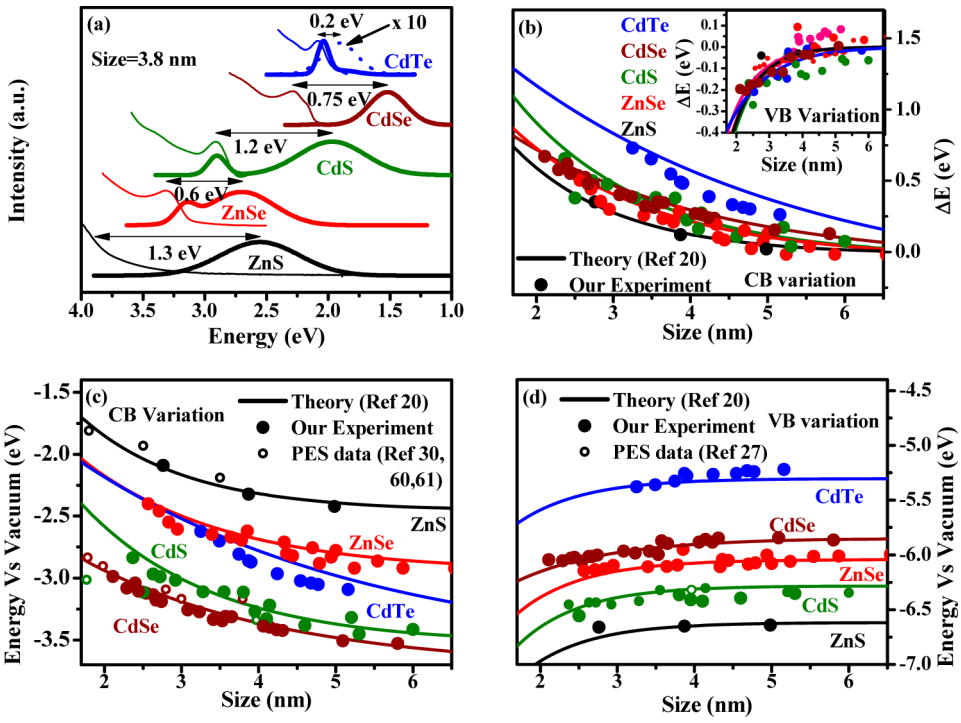

Figure 5. (a) Typical absorption and PL spectra of the 3.8 nm Cu doped II−VI semiconductor nanocrystals showing a shift in the Cu related emission position. (b) Universal curve to study the relative alignment of band offsets as a function of size in various semiconductors for the CB (main panel) and the VB (inset). (c and d) Relative band alignment of various II−VI semiconductors as a function of size for the CB and VB, respectively. The solid line represents the TB theoretical data (ref 20) while the open circles represent the data obtained from literature.[27,30,60,61].

Cu to Cd ratio was a direct result of the onset of precipitation. Surprisingly, contrary to the expectations, the QY of the Cu related emission decreases drastically with increasing stoichiometric percentage of Cu. However, it is also known in the literature that the entire amount of Cu injected is rarely incorporated into the lattice. Hence we performed ICP−OES measurements to determine the actual amount of Cu incorporated within the nanocrystal after washing the samples several times to remove the Cu ions that are not intercalated within the lattice of the nanocrystal and are shown in the inset to Figure 7a. These data show that, though the amount of Cu intercalated into the system is much lower than the stoichiometric concentration, not surprisingly the actual concentration increases with increasing stoichiometric concentration. This suggests that the QY of the Cu related emission is not solely determined by the amount of Cu present within the nanocrystal but also based on surface electronic structure of the host nanocrystal. To have a better understanding of the role of surface on the Cu related emission, for the rest of the studies described in this manuscript, we have used a constant Cu to Cd stoichiometric ratio of 0.25%. Figure 7b shows the area normalized PL spectra obtained using the same Cu concentration with changing TOP amounts during the formation of CdSe. From the figure it is clear that ratio of excitonic to Cu related emission peak varies drastically as a function of TOP concentration. The amount of Cu present in these samples giving rise to such widely varying intensities of the Cu related emission as obtained using ICP−OES was found to be similar within the experimental error. To get a more accurate quantitative estimate of the PL emission, we calculated the absolute QY of the BE emission and the Cu related emission that is plotted for two different concentrations of OlAc in Figure 7c along with QY of the undoped species obtained using similar reaction conditions. By studying the variation of QY of the BE emission in the doped and undoped sample as seen in Figure 7c, it is evident that the QY of the BE emission in the doped sample is similar to that of the undoped sample. However, in the case of the doped sample synthesized using 3 mmol of OlAc, in addition to the ~3% QY of the BE emission, there exists another brighter peak related to Cu emission with QY decreasing monotonically from ~30% to ~10% with increasing TOP concentration. This is a clear indication of a decrease in the number of surface hole traps with increasing TOP concentration and hence suggesting that TOP mainly acts as a hole passivating agent. It is important to note that the Cu related emission does not arise at the cost of the BE emission, since the QY of the BE emission before and after doping is relatively unchanged, but rather happens independently. This further corroborates the theory that the Cu emission can only be seen in the presence of surface hole traps, whereas the BE emission would be absent in presence

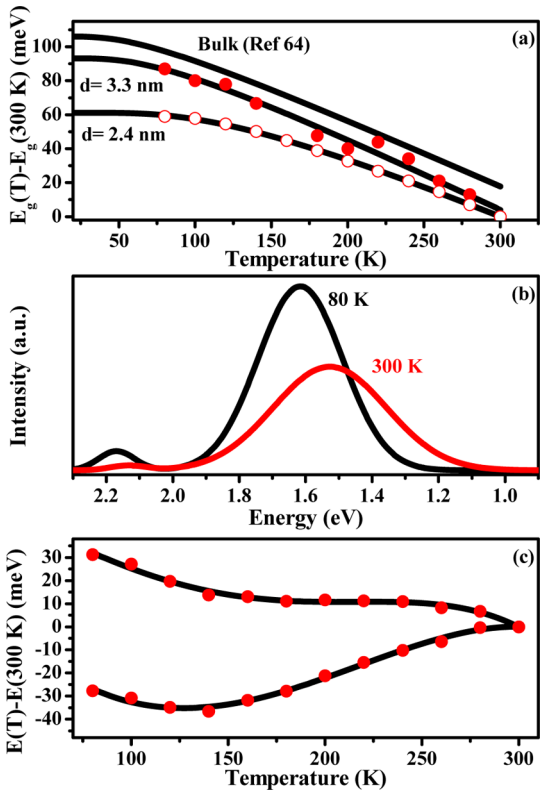

Figure 6. (a) Variation of the excitonic band gap as a function of temperature for two different sizes along with their fits to eq 1 in the text. It also shows the simulated curve for bulk values from literature.[64] (b) Typical PL spectra of 2.4 nm Cu doped CdSe nanocrystals at room temperature and at 80 K. (c) Variation of the CB and VB as a function of temperature for the 2.4 nm CdSe nanocrystal.

of either surface hole or electron traps. However, in the case of 4.5 mmol of OlAc, we observe that the QY of the Cu related emission is non-monotonic suggesting the interaction of OlAc with the TOP molecules in creating surface electron and hole traps. In the presence of a large amount of OlAc and a small amount of TOP, TOP also acts as an electron trap creator and hence the QY of both the Cu related emission and the BE emission decreases in the presence of low TOP and high OlAc concentration.

While the study of QY of the Cu related emission provides us with information on the surface hole traps, study of the fast component of the PL lifetime of the Cu related emission should be an ideal tool to study the surface electron traps since Cu related emission occurs without the involvement of the photogenerated hole. Typical decay plots of Cu related emission for varying concentrations of TOP are shown in Supporting Information, Figure S3a. The percentage of the fast multiexponential component while analyzing PL decay kinetics of the Cu related emission approximated as a biexponential fitting function is shown in the inset to Figure 7c and illustrates a monotonic increase with increasing TOP concentration for high OlAc concentration while it is almost constant for low OlAc concentration. The increase in the fast component implies an increase in the surface electron traps while proving that TOP not only acts as a hole passivating agent but is also a mild creator of electron traps, especially in the presence of other hole passivating agents like OlAc. However, when low OlAc concentration is used, the effect on the electron traps is minimal in agreement with the QY data.

This in turn leads us to the question of the role of OlAc in the passivation surface traps and hence a similar analysis was carried out for a given TOP concentration with varying OlAc concentrations. The results are summarized in Figure 7d. From the figure, it can be seen that the QY of the BE emission of the doped and undoped species are similar showing almost no change with changing OlAc concentrations, which indicates that the electron and hole traps are not simultaneously being passivated by OlAc. Study of Cu related emission however shows a strong monotonic decrease in QY suggesting that OlAc is indeed passivating the hole traps while possibly being insensitive to electron traps. This is further corroborated by looking at the lifetime decay data in Supporting Information, Figure S3b and the fast component of the PL decay kinetics of the Cu related emission shown in the inset to Figure 7d. Since OlAc has no effect on the electron traps, we observe that the percentage of the fast component remains unchanged with increasing OlAc concentration.

In the backdrop of these studies, it is easy to understand the surprising results obtained in Figure 7a. Decreasing QY of the Cu related emission with increasing Cu concentration suggests that Cu precursors are possibly acting as hole passivating agents. Given that stearic acid is used during the synthesis of $CuSt_2$, it can be expected that despite multiple washings, some trace amounts of stearic acid continues to be present in $CuSt_2$. Since increasing the concentration of Cu is achieved by increasing the amount of $CuSt_2$ injected, the amount of stearic acid injected into the reaction mixture increases. As has been observed in the case of OlAc, increasing the presence of acids acts as good hole passivators for the CdSe nanocrystals, and hence there is a decrease in the QY of the Cu emission.

It is also interesting to note that in Figure 6b, the relative intensities of the two bands vary drastically. From the above discussion, it is clear that the intensity of the excitonic peak is determined by the inefficiency of trapping the electron and the hole in the trap states while that of the Cu related band is determined from the efficiency of trapping the hole in the trap states. Since efficiency of trapping charge carriers in the surface trap states are known to exponentially decrease with temperature, the BE emission would be expected to be more dominant at lower temperatures than at room temperature as observed in Figure 6b. However, the QY of the Cu related emission is more complicated since it increases in the absence of electron trap states and the presence of hole trap states, that is till now, not

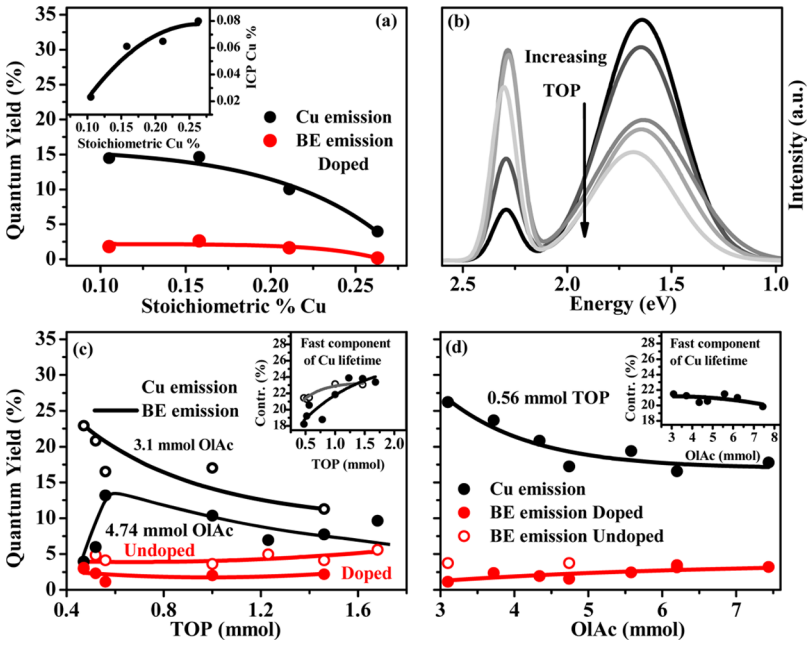

Figure 7. (a) Variation of QY with increasing Cu content in the nanocrystal. The inset shows the actual Cu/Cd ratio as a function of stoichiometric Cu added during the synthesis. (b) Typical PL spectra of Cu doped CdSe nanocrystals with similar Cu content but synthesized with different TOP concentrations. Variation of the QY of the Cu related emission and BE emission for both doped and undoped species as a function of (c) TOP concentration for two different concentrations of OlAc and (d) OlAc concentration for a given TOP concentration. The insets show the variation of the percentage of the fast components of the lifetime of the Cu peak with varying TOP concentration and OlAc concentration.

well studied at varying temperatures due to the absence of probes to study these trap states separately.

Thus from these studies it is evident that it is possible to study the passivation of the electron and hole traps using the internal Cu related emission. The QY of the undoped sample is known to be further enhanced by systematically introducing other passivating agents like amine and trioctylphosphine oxide as discussed earlier. However since the goal of this manuscript is to show the proof of principle, we have not performed an extensive study by introducing the other passivating agents.

CONCLUSION

We have shown that it is indeed possible to dope CdSe with Cu and obtain the Cu related emission by systematically increasing the hole traps within the system, and the earlier reported failures were mainly due to the absence of surface hole traps. We have used Cu doping to study the variation of CB and VB as a function of size and temperature in the nanocrystals using CdSe as a model system. This study has been further extended to different sizes of other semiconductors leading to the relative band alignment in nanocrystals for the first time as well as studying the variation of CB and VB as a function of temperature. Further we have also used the QY and PL decay kinetics of the Cu related emission to study the surface of the nanocrystal. Thus we show that by appropriately studying the mechanism of the Cu related emission it is possible to dope Cu in any nanocrystal and study the bulk and surface electronic structure of the nanocrystal using Cu d level as an internal standard or a nanosensor.

METHODS

Materials. Cadmium oxide (CdO), stearic acid and copper(II) acetate monohydrate were purchased from S D Fine chemicals. OlAc (90%), 1-octadecene (ODE, 90%), octadecylamine (ODA, 97%), trioctyl phosphine oxide (TOPO, 90%), trioctylphosphine (TOP, 90%), and Se pellets were obtained from Sigma Aldrich. Tetramethyl ammonium hydroxide pentahyrate (TMAH, 98%) was obtained from Spectrochem. All purchased chemicals were used without further purification. Copper stearate ($CuSt_2$) was synthesized and purified similar to the literature reports published previously. Briefly, $CuAc_2$ was dissolved in methanol and added dropwise to a flask containing TMAH and OlAc to obtain precipitates of $CuSt_2$ that were thoroughly washed with methanol and acetone.

CdSe nanocrystals were synthesized using two different techniques to study the effect of surface passivation. For both these methods, $CdOl_2$ was synthesized using modified literature methods. Briefly, CdO, OlAc, and ODE (4.5 mL) were degassed in vacuum and backfilled with Ar and heated to high temperature in argon atmosphere till the solution turns colorless. To study the surface effects, $CdOl_2$ with different molarities were prepared by varying the weight ratios of CdO to OlAc (1:2.5−1:5). 2 M TOPSe solution was prepared by dissolving an appropriate amount of Se in TOP in a glovebox. It was then further diluted with TOP to obtain different molarities (1.2−0.33 M) of the solution

Standard synthesis of CdSe nanocrystals was carried out by degassing ODE (5 mL), ODA (1.5 g), and TOPO (650 mg) in a three necked flask in vacuum and backfilling with Ar. To this solution, 1 mL of 0.83 M cadmium oleate was injected at 100 °C in argon atmosphere followed by addition of 1.5 mL of TOPSe (1 M) at 210 °C. This solution was heated at 210 °C for a minute

and then cooled to 140 °C in order to avoid the further growth of CdSe nanocrystals. To this solution, 50 μmol $Cu(St)_2$ solution in 2 mL of ODE was added to the reaction mixture and annealed for 20 min to obtain Cu-doped nanocrystals. In the undoped case, instead of the $CuSt_2$ solution of ODE, only ODE was added as a blank and was annealed for similar length of time. Samples were washed with a hexane methanol mixture and precipitated using ethanol.

Low Ligand Method. An appropriate solution of $CdOl_2$ and ODE were degassed in a three necked flask and heated to 180 °C. TOPSe (0.47−1.68 mmol TOP/0.0197 g Se) was injected at 180 °C in argon atmosphere and annealed for 1 min to form CdSe nanocrystals. The reaction was cooled down to 140 °C and a $CuSt_2$ solution of different molarities was added dropwise and annealed for 20 min. Samples were washed with a hexane methanol mixture and precipitated using ethanol. To obtain the bigger sizes, the reaction mixture was heated to a higher temperature after 20 min with additional injection of $CdOl_2$ precursor.

Synthesis of Other Cu Doped II−VI Semiconductors. Cu doped CdS nanocrystals were synthesized by first preparing the different sizes of CdS nanocrystals using an already reported method in literature.[65] Following the formation of CdS nanocrystals, 10 μmoles of $Cu(St)_2$ solution in 1 mL of ODE was added at 150 °C and maintained for 2 h at that temperature to obtain Cu doped CdS nanocrystals of different sizes. Cu doped CdTe nanocrystals were synthesized by preparing CdTe nanocrystals of different sizes as reported in literature[66] followed by cooling the reaction mixture to 160 °C. At this temperature, 50 μmoles of copper acetate in 0.5 mL of oleylamine was added as the copper precursor[36] to the reaction mixture in order to obtain Cu doped CdTe nanocrystals of various sizes. Samples thus obtained were washed with a mixture of hexane and methanol and then precipitated using acetone. Cu doped ZnS and Cu doped ZnSe nanocrystals were synthesized using the methods reported in literature.[35,67]

Characterization and Spectroscopic Studies. Inductively coupled plasma optical emission spectroscopy (ICP−OES) was used to determine the Cu to Cd ratio in the doped nanocrystals. Nanocrystals were washed several times with methanol and once with ethanol to remove excess precursors and then digested in concentrated HNO_3 and diluted with Millipore water. ICP−OES was carried out using a Perkin-Elmer Optima 7000 DV instrument.

Nanocrystal structure and size identification of the particles were carried out using X-ray diffraction and transmission electron microscopy. TEM images were recorded using Technai F30 UHR version electron microscope, using a field emission gun (FEG) at an accelerating voltage of 300 kV. Samples for TEM were prepared by adding a solution of the nanocrystals dissolved in hexane dropwise on carbon coated Cu grid. The solution was allowed to evaporate leaving behind the nanocrystals. Crystal structure identification of the particles was carried out using X-ray diffraction, recorded on Bruker D8 Advance diffractometer using Cu Kα radiation. Since the diffracted intensities from these nanocrystals are generally weak, all patterns were recorded at a slow scan rate (0.75° per minute) in order to get a high signal-to-noise ratio. The bulk XRD was obtained from the inorganic crystal structure database and broadened using the Scherrer formula to simulate the corresponding nanocrystal XRD.

UV−visible absorption spectra of various aliquots dissolved in hexane were obtained using Agilent 8453 UV−visible spectrometer. Steady state PL spectra were collected using the 450 W xenon lamp as the source on the FLSP920 spectrometer, Edinburgh Instruments, while the lifetime measurements were carried out on an EPL-405 ps. A pulsed diode laser was used as excitation source (λ_{ex} = 405 nm). Absolute PL QY was determined using an integrating sphere for both doped and undoped samples. Low temperature measurements were performed using an Oxford DN2 liquid nitrogen cryostat with the same spectrometer.

Conflict of Interest: The authors declare no competing financial interest.

Supporting Information Available: XRD patterns of Cu doped CdSe with high ligand concentration, PL correction, table documenting the dopant PL positions in various NC systems available in the literature, and the lifetime decay curves for the Cu related emission. This material is available free of charge *via* the Internet at http://pubs.acs.org.

Acknowledgment. We thank JNCASR and the Department of Science and Technology, Government of India, for financial support. G.K.G. thanks CSIR for a research fellowship. We would like to thank Mr. Karthick Bala and Dr. Ranjan Datta for the TEM measurements and Mr. J. Pratap for the photographs of the nanocrystal emission.

REFERENCES AND NOTES

1. Ellingson, R. J.; Beard, M. C.; Johnson, J. C.; Yu, P.; Micic, O. I.; Nozik, A. J.; Shabaev, A.; Efros, A. L. Highly Efficient Multiple Exciton Generation in Colloidal PbSe and PbS Quantum Dots. *Nano Lett.* **2005**, *5*, 865–871.
2. Carlson, B.; Leschkies, K.; Aydil, E. S.; Zhu, X. Y. Valence Band Alignment at Cadmium Selenide Quantum Dot and Zinc Oxide (1010) Interfaces. *J. Phys. Chem. C* **2008**, *112*, 8419–8423.
3. Sun, L.; Choi, J. J.; Stachnik, D.; Bartnik, A. C.; Hyun, B. R.; Malliaras, G. G.; Hanrath, T.; Wise, F. W. Bright Infrared Quantum-Dot Light-Emitting Diodes through Inter-dot Spacing Control. *Nat. Nanotechnol.* **2011**, *7*, 369–373.
4. Kongkanand, A.; Tvrdy, K.; Takechi, K.; Kuno, M.; Kamat, P. V. Quantum Dot Solar Cells. Tuning Photoresponse through Size and Shape Control of CdSe−TiO_2 Architecture. *J. Am. Chem. Soc.* **2008**, *130*, 4007–4015.
5. Kamat, P. V. Quantum Dot Solar Cells. Semiconductor Nanocrystals as Light Harvesters. *J. Phys. Chem. C* **2008**, *112*, 18737–18753.
6. Pradhan, N.; Reifsnyder, D.; Xie, R.; Aldana, J.; Peng, X. Surface Ligand Dynamics in Growth of Nanocrystals. *J. Am. Chem. Soc.* **2007**, *129*, 9500–9509.
7. Nag, A.; Hazarika, A.; Shanavas, K. V.; Sharma, S. M.; Dasgupta, I.; Sarma, D. D. Crystal Structure Engineering by Fine-Tuning the Surface Energy: The Case of CdE (E = S/Se) Nanocrystals. *J. Phys. Chem. Lett.* **2011**, *2*, 706–712.
8. Schapotschnikow, P.; Hommersom, B.; Vlugt, T. J. H. Adsorption and Binding of Ligands to CdSe Nanocrystals. *J. Phys. Chem. C* **2009**, *113*, 12690–12698.
9. Ji, X.; Copenhaver, D.; Sichmeller, C.; Peng, X. Ligand Bonding and Dynamics on Colloidal Nanocrystals at Room Temperature: The Case of Alkylamines on CdSe Nanocrystals. *J. Am. Chem. Soc.* **2008**, *130*, 5726–5735.
10. Viswanatha, R.; Sarma, D. D. Study of the Growth of Capped ZnO Nanocrystals: A Route to Rational Synthesis. *Chem.—Eur. J.* **2006**, *12*, 180–186.
11. Sewall, S. L.; Cooney, R. R.; Anderson, K. E. H.; Dias, E. A.; Sagar, D. M.; Kambhampati, P. State-Resolved Studies of Biexcitons and Surface Trapping Dynamics in Semiconductor Quantum Dots. *J. Chem. Phys.* **2008**, *129*, 084701.
12. Tyagi, P.; Kambhampati, P. False Multiple Exciton Recombination and Multiple Exciton Generation Signals in Semiconductor Quantum Dots Arise from Surface Charge Trapping. *J. Chem. Phys.* **2011**, *134*, 094706.
13. Cooney, R. R.; Sewall, S. L.; Sagar, D. M.; Kambhampati, P. State-Resolved Manipulations of Optical Gain in Semiconductor Quantum Dots: Size Universality, Gain Tailoring, and Surface Effects. *J. Chem. Phys.* **2009**, *131*, 164706.
14. Banerjee, S.; Maity, S.; Datta, A. Enhanced Trapping Efficiency in Acid-Treated Silica Nanostructures. *J. Phys. Chem. C* **2011**, *115*, 22804–22809.
15. Yu, W. W.; Qu, L.; Guo, W.; Peng, X. Experimental Determination of the Extinction Coefficient of CdTe, CdSe, and CdS Nanocrystals. *Chem. Mater.* **2003**, *15*, 2854–2860.
16. Poznyak, S. K.; Osipovich, N. P.; Shavel, A.; Talapin, D. V.; Gao, M.; Eychmueller, A.; Gaponik, N. Size-Dependent Electrochemical Behavior of Thiol-Capped CdTe Nanocrystals in Aqueous Solution. *J. Phys. Chem. B* **2005**, *109*, 1094–1100.
17. Kucur, E.; Riegler, J.; Urban, G. A.; Nann, T. Determination of Quantum Confinement in CdSe Nanocrystals by Cyclic Voltammetry. *J. Chem. Phys.* **2003**, *119*, 2333.

18. Haram, S. K.; Kshirsagar, A.; Gujarathi, Y. D.; Ingole, P. P.; Nene, O. A.; Markad, G. B.; Nanavati, S. P. Quantum Confinement in CdTe Quantum Dots: Investigation through Cyclic Voltammetry Supported by Density Functional Theory (DFT). *J. Phys. Chem. C* **2011**, *115*, 6243–6249.
19. Jasieniak, J.; Califano, M.; Watkins, S. Size-Dependent Valence and Conduction Band-Edge Energies of Semiconductor Nanocrystals. *ACS Nano* **2011**, *5*, 5888–5902.
20. Viswanatha, R.; Sarma, D. D. Effect of Structural Modification on the Quantum Size Effect in II−VI Semiconducting Nanocrystals. *Chem. Asian J.* **2009**, *4*, 904–909.
21. Viswanatha, R.; Sapra, S.; Saha-Dasgupta, T.; Sarma, D. D. Electronic Structure of and Quantum Size Effect in III−V and II−VI Semiconducting Nanocrystals using a Realistic Tight Binding Approach. *Phys. Rev. B* **2005**, *72*, 045333.
22. Hu, J.; Wang, L.; Li, L.; Yang, W.; Alivisatos, A. P. Semiempirical Pseudopotential Calculation of Electronic States of CdSe Quantum Rods. *J. Phys. Chem. B* **2002**, *106*, 2447–2452.
23. Bernard, J. E.; Zunger, A. Electronic Structure of ZnS, ZnSe, ZnTe, and Their Pseudobinary Alloys. *Phys. Rev. B* **1987**, *36*, 3199.
24. Franceschetti, A.; Fu, H.; Wang, L. W.; Zunger, A. Many-Body Pseudopotential Theory of Excitons in InP and CdSe Quantum Dots. *Phys. Rev. B* **1999**, *60*, 1819–1829.
25. Jasieniak, J.; Smith, L.; Embden, J. v.; Mulvaney, P.; Califano, M. Re-examination of the Size-Dependent Absorption Properties of CdSe Quantum Dots. *J. Phys. Chem. C* **2009**, *113*, 19468–19474.
26. Santra, P. K.; Viswanatha, R.; Daniels, S. M.; Pickett, N. L.; Smith, J. M.; O' Brien, P.; Sarma, D. D. Investigation of the Internal Heterostructure of Highly Luminescent Quantum Dot-Quantum Well Nanocrystals. *J. Am. Chem. Soc.* **2008**, *131*, 470–477.
27. Colvin, V. L.; Alivisatos, A. P.; Tobin, J. G. Valence-Band Photoemission from a Quantum-Dot System. *Phys. Rev. Lett.* **1991**, *66*, 2786–2789.
28. Nanda, J.; Kuruvilla, B. A.; Sarma, D. D. Photoelectron Spectroscopic Study of CdS Nanocrystallites. *Phys. Rev. B* **1999**, *59*, 7473.
29. Van Buuren, T.; Dinh, L. N.; Chase, L. L.; Siekhaus, W. J.; Terminello, L. J. Changes in the Electronic Properties of Si Nanocrystals as a Function of Particle Size. *Phys. Rev. Lett.* **1998**, *80*, 3803–3806.
30. Lee, J. R. I.; Meulenberg, R. W.; Hanif, K. M.; Mattoussi, H.; Klepeis, J. E.; Terminello, L. J.; van Buuren, T. Experimental Observation of Quantum Confinement in the Conduction Band of CdSe Quantum Dots. *Phys. Rev. Lett.* **2007**, *98*, 146803.
31. Alperson, B.; Rubinstein, I.; Hodes, G.; Porath, D.; Millo, O. Energy Level Tunneling Spectroscopy and Single Electron Charging in Individual CdSe Quantum Dots. *Appl. Phys. Lett.* **1999**, *75*, 1751.
32. Choi, H. J.; Yang, J. K.; Park, H. H. Effect of Surface Capping Molecules on the Electronic Structure of CdSe Nanocrystal Film. *Thin Solid Films* **2006**, *494*, 207–210.
33. Choi, H. J.; Yang, J. K.; Yoon, S.; Park, H. H. Changes in the Electronic Energy Structure of CdSe Nanocrystals of Close-Packed Array by *in-Situ* Annealing. *Appl. Surf. Sci.* **2005**, *244*, 92–95.
34. Passler, R.; Griebl, E.; Riepl, H.; Lautner, G.; Bauer, S.; Preis, H.; Gebhardt, W.; Buda, B.; As, D. J.; Schikora, D. Temperature Dependence of Exciton Peak Energies in ZnS, ZnSe, and ZnTe Epitaxial Films. *J. Appl. Phys.* **1999**, *86*, 4403.
35. Chen, D.; Viswanatha, R.; Ong, G. L.; Xie, R.; Balasubramaninan, M.; Peng, X. Temperature Dependence of Elementary Processes in Doping Semiconductor Nanocrystals. *J. Am. Chem. Soc.* **2009**, *131*, 9333–9339.
36. Karan, N. S.; Sarma, D. D.; Kadam, R. M.; Pradhan, N. Doping Transition Metal (Mn or Cu) Ions in Semiconductor Nanocrystals. *J. Phys. Chem. Lett.* **2010**, *1*, 2863–2866.
37. Pradhan, N.; Goorskey, D.; Thessing, J.; Peng, X. An Alternative of CdSe Nanocrystal Emitters: Pure and Tunable Impurity Emissions in ZnSe Nanocrystals. *J. Am. Chem. Soc.* **2005**, *127*, 17586–17587.
38. Viswanatha, R.; Brovelli, S.; Pandey, A.; Crooker, S. A.; Klimov, V. I. Copper-Doped Inverted Core/Shell Nanocrystals with Permanent Optically Active Holes. *Nano Lett.* **2011**, *11*, 4753–4758.
39. Srivastava, B. B.; Jana, S.; Pradhan, N. Doping Cu in Semiconductor Nanocrystals: Some Old and Some New Physical Insights. *J. Am. Chem. Soc.* **2011**, *133*, 1007–1015.
40. Xie, R.; Peng, X. Synthesis of Cu-Doped InP Nanocrystals (d-dots) with ZnSe Diffusion Barrier as Efficient and Color-Tunable NIR Emitters. *J. Am. Chem. Soc.* **2009**, *131*, 10645–10651.
41. Su, F. H.; Fang, Z. L.; Ma, B. S.; Ding, K.; Li, G. H.; Xu, S. J. Temperature and Pressure Behavior of the Emission Bands from Mn-, Cu-, and Eu-Doped ZnS Nanocrystals. *J. Appl. Phys.* **2004**, *95*, 3344–3349.
42. Du, Y. P.; Zhang, Y. W.; Sun, L. D.; Yan, C. H. Efficient Energy Transfer in Monodisperse Eu-Doped ZnO Nanocrystals Synthesized from Metal Acetylacetonates in High-Boiling Solvents. *J. Phys. Chem. C* **2008**, *112*, 12234–12241.
43. Wang, L.; Li, Y. Controlled Synthesis and Luminescence of Lanthanide Doped $NaYF_4$ Nanocrystals. *Chem. Mater.* **2007**, *19*, 727–734.
44. Ishizumi, A.; Kanemitsu, Y. Structural and Luminescence Properties of Eu-Doped ZnO Nanorods Fabricated by a Microemulsion Method. *Appl. Phys. Lett.* **2005**, *86*, 253106–253106−3.
45. Schwartz, D. A.; Norberg, N. S.; Nguyen, Q. P.; Parker, J. M.; Gamelin, D. R. Magnetic Quantum Dots: Synthesis, Spectroscopy, and Magnetism of Co^{2+}-and Ni^{2+}-Doped ZnO Nanocrystals. *J. Am. Chem. Soc.* **2003**, *125*, 13205–13218.
46. Norberg, N. S.; Dalpian, G. M.; Chelikowsky, J. R.; Gamelin, D. R. Energetic Pinning of Magnetic Impurity Levels in Quantum-Confined Semiconductors. *Nano Lett.* **2006**, *6*, 2887–2892.
47. Norris, D. J.; Yao, N.; Charnock, F. T.; Kennedy, T. A. High-Quality Manganese-Doped ZnSe Nanocrystals. *Nano Lett.* **2001**, *1*, 3–7.
48. Nag, A.; Chakraborty, S.; Sarma, D. D. To Dope Mn^{2+} in a Semiconducting Nanocrystal. *J. Am. Chem. Soc.* **2008**, *130*, 10605–10611.
49. Sapra, S.; Sarma, D. D.; Sanvito, S.; Hill, N. A. Influence of Quantum Confinement on the Electronic and Magnetic Properties of (Ga,Mn) as Diluted Magnetic Semiconductor. *Nano Lett.* **2002**, *2*, 605–608.
50. Ture, I. E.; Poulin, F.; Brinkman, A. W.; Woods, J. Electron Traps and Deep Levels in Cadmium Selenide. *Phys. Stat. Sol. A* **1983**, *77*, 535–544.
51. Norris, D. J.; Efros, A. L.; Erwin, S. C. Doped Nanocrystals. *Science* **2008**, *319*, 1776–1779.
52. Van de Walle, C. G.; Neugebauer, J. Universal Alignment of Hydrogen Levels in Semiconductors, Insulators and Solutions. *Nature* **2003**, *423*, 626–628.
53. Grimmeiss, H. G.; Ovren, C.; Ludwig, W.; Mach, R. Identification of Deep Centers in ZnSe. *J. Appl. Phys.* **1977**, *48*, 5122–5126.
54. Laurenti, J. P.; Bastide, G.; Rouzeyre, M.; Triboulet, R. Localized Defects in p-CdTe:Cu Doped by Copper Incorporation During Bridgman Growth. *Solid State Commun.* **1988**, *67*, 1127–1130.
55. Shionoya, S.; Koda, T.; Era, K.; Fujiwara, H. Nature of Luminescence Transitions in ZnS Crystals. *J. Phys. Soc. Jpn.* **1964**, *19*, 1157–1167.
56. Ture, I. E.; Claybourn, M.; Brinkman, A. W.; Woods, J. Copper Centers in CdSe. *J. Appl. Phys.* **1986**, *60*, 1670–1675.
57. Erwin, S. C.; Zu, L.; Haftel, M. I.; Efros, A. L.; Kennedy, T. A.; Norris, D. J. Doping Semiconductor Nanocrystals. *Nature* **2005**, *436*, 91–94.
58. Viswanatha, R.; Sapra, S.; Gupta, S. S.; Satpati, B.; Satyam, P. V.; Dev, B. N.; Sarma, D. D. Synthesis and Characterization of Mn-Doped ZnO Nanocrystals. *J. Phys. Chem. B* **2004**, *108*, 6303–6310.
59. Lakowicz, J. R. *Principles of Fluorescence Spectroscopy*, 3rd ed.; Springer Publications: New York, 2006; p 954.
60. Sapra, S. *Experimental and Theoretical Investigations of the Electronic and Optical Properties of Semiconductor Nanocrystals*; Indian Institute of Science, Bangalore, India, 2003.

61. Luning, J.; Rockenberger, J.; Eisebitt, S.; Rubensson, J. E.; Karl, A.; Kornowski, A.; Weller, H.; Eberhardt, W. Soft X-ray Spectroscopy of Single Sized CdS Nanocrystals: Size Confinement and Electronic Structure. *Solid State Commun.* **1999**, *112*, 5–9.
62. Brovelli, S.; Galland, C.; Viswanatha, R.; Klimov, V. I. Tuning Radiative Recombination in Cu-Doped Nanocrystals *via* Electrochemical Control of Surface Trapping. *Nano Lett.* **2012**, *12*, 4372.
63. Perna, G.; Lastella, M.; Ambrico, M.; Capozzi, V. Temperature Dependence of the Optical Properties of ZnSe Films Deposited on Quartz Substrate. *Appl. Phys. A: Mater. Sci. Process.* **2006**, *83*, 127–130.
64. Logothetidis, S.; Cardona, M.; Lautenschlager, P.; Garriga, M. Temperature Dependence of the Dielectric Function and the Interband Critical Points of CdSe. *Phys. Rev. B* **1986**, *34*, 2458.
65. Yu, W. W.; Peng, X. Formation of High-Quality CdS and Other II−VI Semiconductor Nanocrystals in Noncoordinating Solvents: Tunable Reactivity of Monomers. *Angew. Chem., Int. Ed.* **2002**, *41*, 2368–2371.
66. Kloper, V.; Osovsky, R.; Kolny-Olesiak, J.; Sashchiuk, A.; Lifshitz, E. The growth of Colloidal Cadmium Telluride Nanocrystal Quantum Dots in the Presence of Cd0 Nanoparticles. *J. Phys. Chem. C* **2007**, *111*, 10336–10341.
67. Srivastava, B. B.; Jana, S.; Karan, N. S.; Paria, S.; Jana, N. R.; Sarma, D. D.; Pradhan, N. Highly Luminescent Mn-Doped ZnS Nanocrystals: Gram-Scale Synthesis. *J. Phys. Chem. Lett.* **2010**, *1*, 1454–1458.